

1 **Mount Pinatubo’s effect on the soil moisture-based drivers to the plant**
2 **productivity**

3
4 Ram Singh^{1,2}, Kostas Tsigaridis^{1,2}, Diana Bull³, Laura P Swiler³, Benjamin M Wagman³, Kate
5 Marvel^{2,1}
6

7 **Affiliations**

8 ¹ *Center for Climate Systems Research, Columbia University, New York, USA*

9 ² *NASA Goddard Institute for Space Studies, New York, NY-10025, USA*

10 ³ *Sandia National Laboratories, Albuquerque, NM, USA*
11

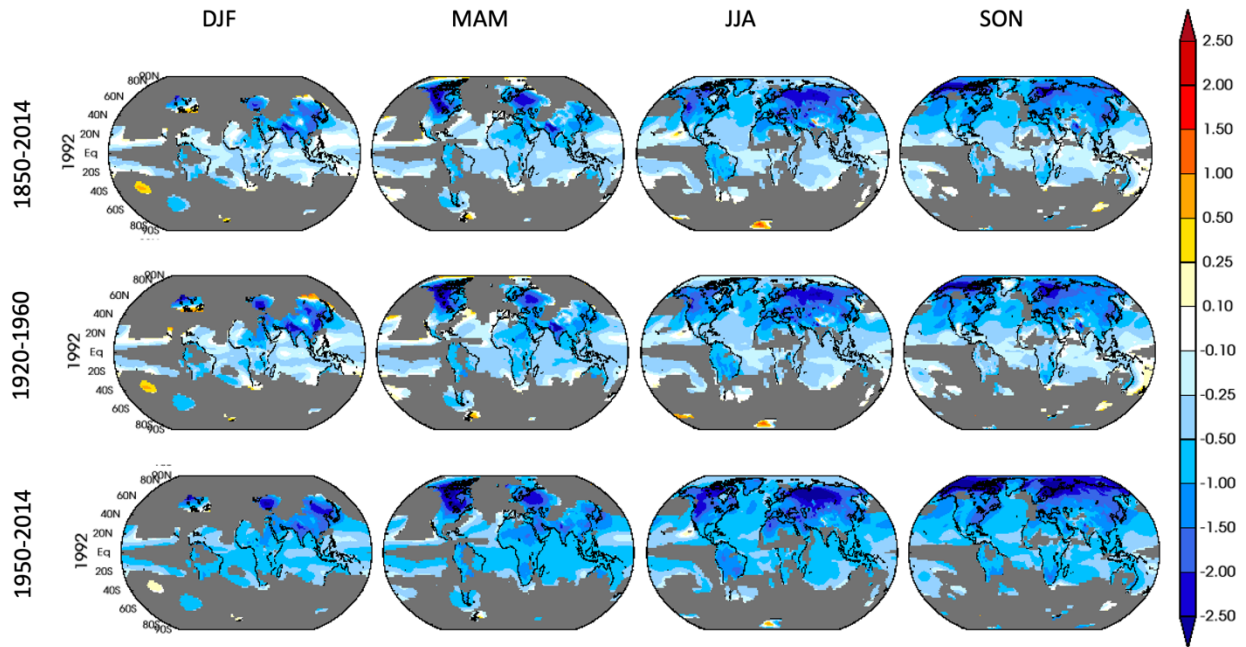
12 **Correspondence:** Ram Singh (rs4068@columbia.edu, ram.bhari85@gmail.com)
13
14

15 **Supplementary Information**
16

17 **S1.0 Reference period selection**

18 The requirement of a baseline time selection points towards a precise representation of
19 climate conditions over a historical period, especially towards the later part of the 20th century,
20 and sufficiently long enough for the calibration of drought indices. Figure S1 compares seasonal
21 surface temperature responses in 1992 with respect to three selected base climate periods. It
22 clearly shows that seasonal surface temperature is considerably influenced by the dominance of
23 no anthropogenic forcing period (1850-2014 and 1920-1960). Consideration of the entire
24 historical (1850-2014) and volcanically quiescent time-slice (1920-1960) as a base period result
25 in the biasing of the reference climate towards the non-anthropogenic emission era.
26 Consequently, the volcano-induced signal due to the Mt. Pinatubo eruption gets muted by the
27 response due to anthropogenic forcings. This influence is minimal with respect to the base period
28 of 1950-2014, as this period mostly covers the period of anthropogenic signal emergence, and its
29 length is sufficient for calibration statistics for SMDI and ETDI (As shown in Figure S1).

30



31

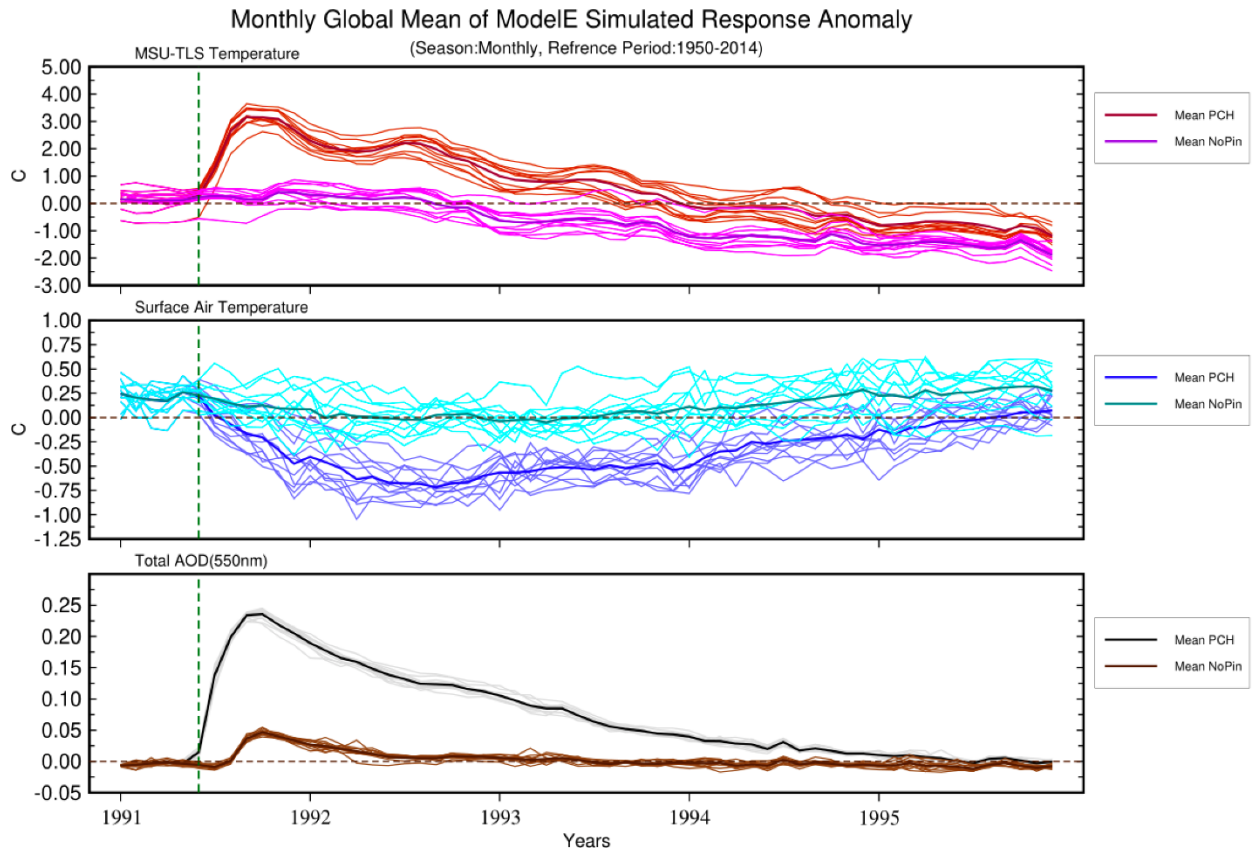
32 Figure S1. Seasonal surface temperature anomaly (multi-ensemble mean) for the year 1992 with
33 respect to three different reference (base) time periods (row-wise).

34

35

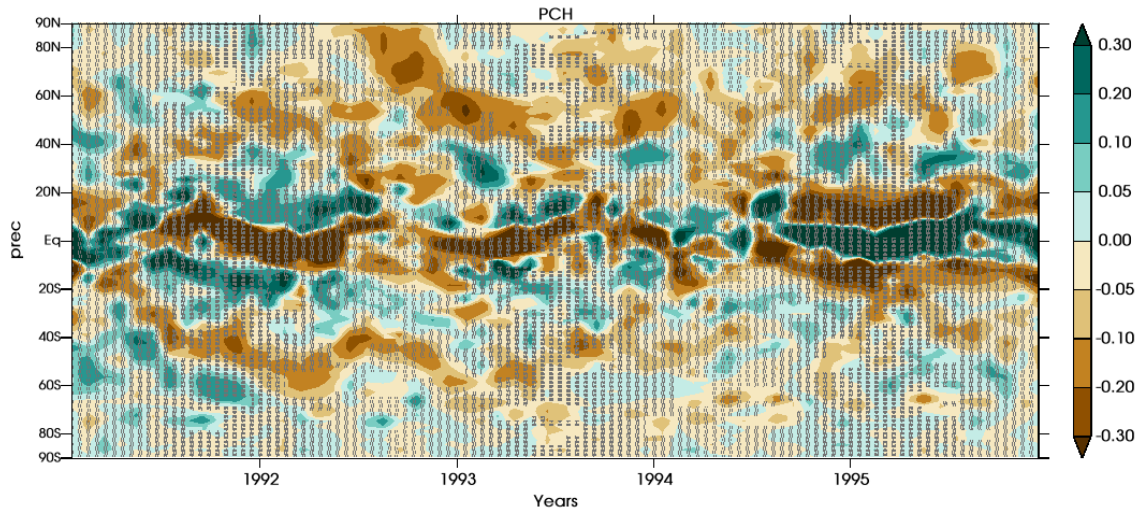
36

37



38
 39
 40
 41
 42
 43
 44
 45
 46
 47
 48
 49
 50

Figure S2: Globally averaged microwave sounding unit temperature (MSU-TLS) for lower stratosphere, surface temperature and total aerosol optical depth (AOD) at 550 nm wavelength response with respect to 1950-2014 as the reference period.



51

52

53 Figure S3: Zonal mean anomaly of rainfall response (mm/day) after the 1991's Mt. Pinatubo
 54 eruption. Grey colored stippling marks the statistically non-significant rainfall signal in
 55 comparison to the counterfactual ensemble.

56

57

58 Close et al., (2016) have postulated that the asymmetrical surface cooling and radiative balance

59 perturbation create an energetical deficit in the hemisphere of eruption and consequently, it

60 constrains the poleward propagation of tropical rainfall belt (ITCZ) in that hemisphere. The

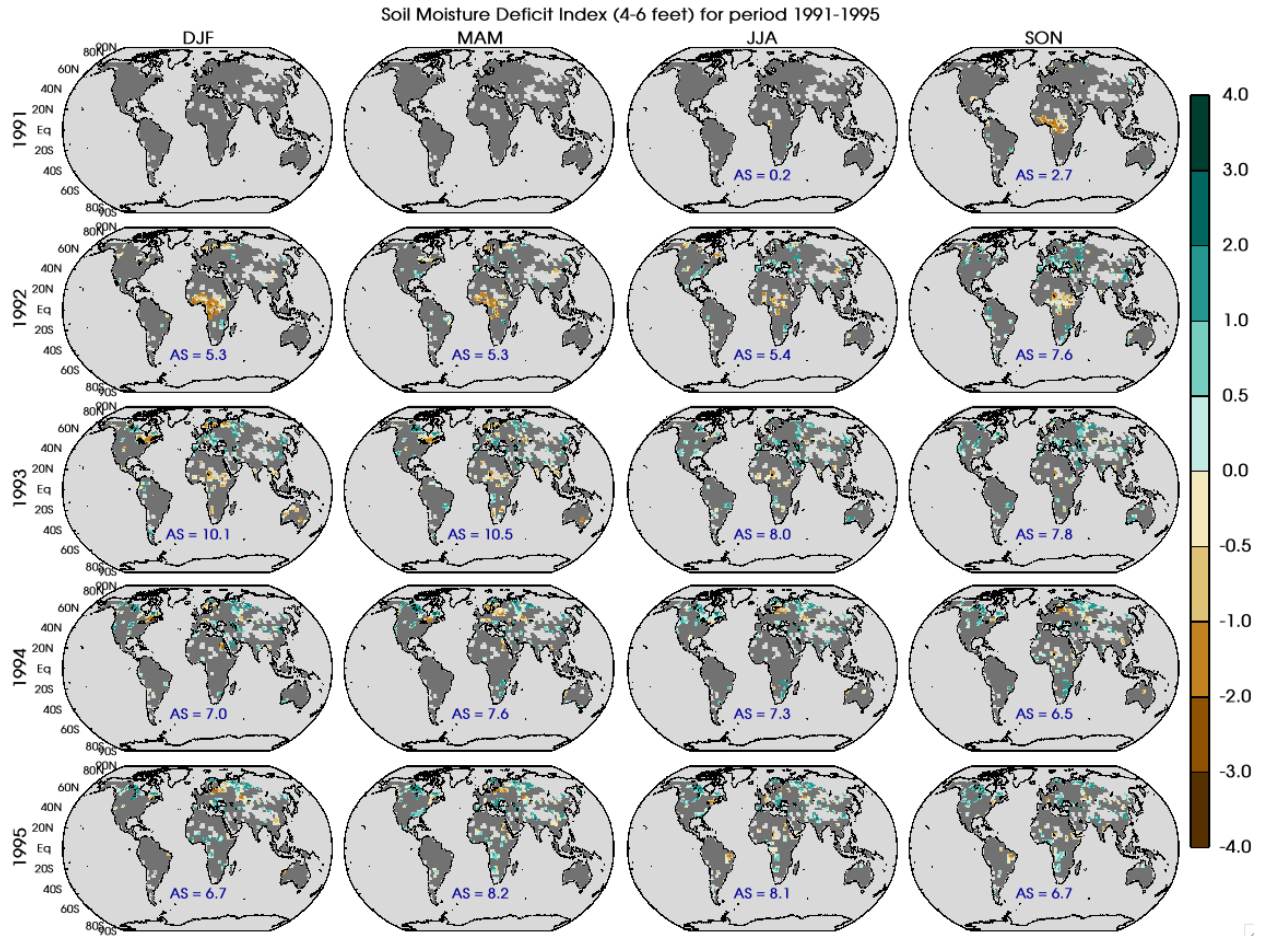
61 zonal mean of the rainfall response (Figure S3) shows a clear decreasing trend in the northern

62 hemisphere tropical and higher latitudes with a positive rainfall response band around 20° N.

63

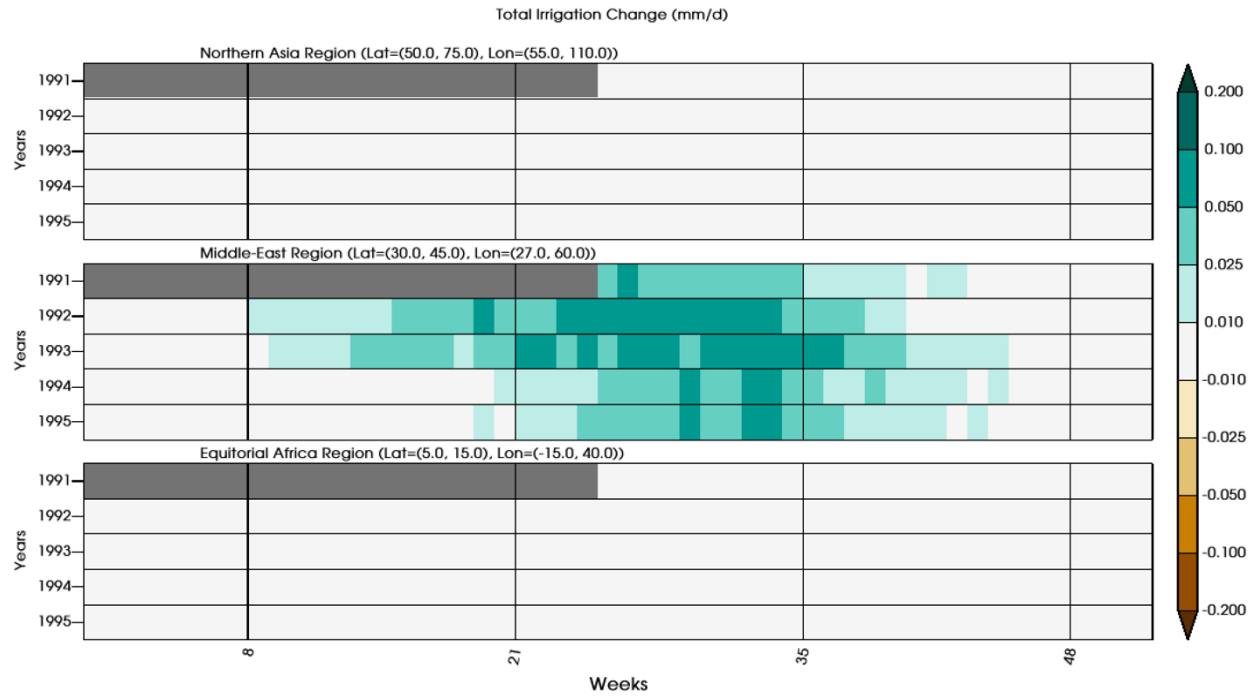
64

65



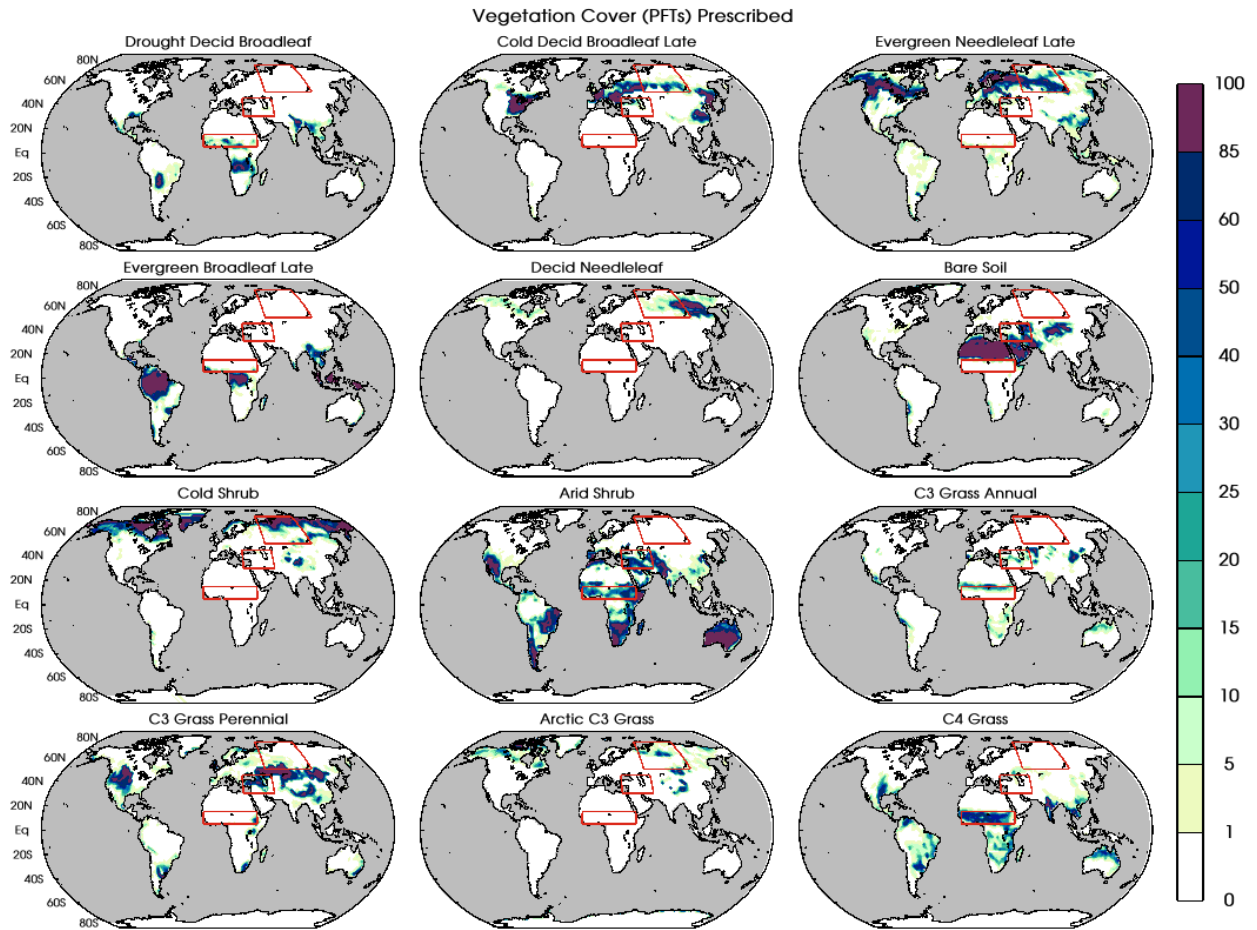
66
67
68
69
70
71
72
73
74
75
76

Fig S4: Soil moisture deficit index (SMDI_6) for the 4-6 feet depth of soil at seasonal scale from the year 1991 to 1995. Grey color is painted over the grid cells where the SMDI_6 is not statistically significant in contrast to counter-factual ensemble. The parameter AS on each panel marks the percentage of land area which shows a statistically significant dry or wet response after the Mt. Pinatubo eruption.



77
78
79
80

Figure S5: - regionally averaged irrigation implemented in GISS modelE2.1 for the years 1991-1995.



81
82

83 Figure S6. Percentage of grid cells for various vegetation plant functional type (PFTs) prescribed
84 to ModelE. Red colored boxes are the various regions selected for the weekly scale analysis of
85 drought metrics.